 CMES, vol.24, no.1, pp.51-60, 2008

Line Search Partitioned Approach for Fluid-structure Interaction Analysis of Flapping Wing

Tomonori Yamada[1] **and Shinobu Yoshimura**[1]

Abstract: Flight dynamics of flapping insects is still an open area of research, though it is well known that they can provide superior flight abilities such as hovering motion. The numerical analysis of flapping wing requires fluid-structure interaction (FSI) analysis to evaluate the effect of deformable wing on flight ability. Such FSI analysis is quite challenging because not only the tight coupling approach to predict flight ability accurately, but also the robust mesh control to trace the large motion of the wing with elastic deformation are required. A new iterative partitioned coupling algorithm for the FSI problems is proposed in this paper. In the proposed approach, non-linearity of the FSI problems is mainly treated on the interface using the line search method, which minimizes non-equilibrated displacements on the interface in each fixed point iteration. This approach is introduced to improve the robustness and efficiency of computation. A two-dimensional FSI analysis of a flapping wing shows that elastic deformation of the wing results in passive feathering motion and generates lift force effectively.

Keyword: Fluid-structure interaction, partitioned method, line search approach, flapping wing.

1 Introduction

Numerical simulation of fluid-structure interaction (FSI) problems arises in many bioengineering fields including blood flow [Yang, Tang, Yuan, Hatsukami, Zheng and Woodard (2007)], crawl swimming [Gardano and Dabnichki (2006)], and bio mimetic robots subjected to fluid flows, such as micro air vehicles (MAV) [Schenato, Wu and Sastry (2004)]. For FSI problems with strong interaction between solid and fluid portions, monolithic approaches [Zhang and Hisada (2001)] [Ishihara and Yoshimura (2005)] are usually adopted as a solution procedure because of its robustness. On the other hand, partitioned coupling schemes, in which solid and fluid analyses are separately conducted, are preferable in terms of their computation efficiency because each physical phenomenon can adopt its most efficient solution procedures, for instance, Balancing Domain Decomposition method [Mandel (1993)] for solid analysis and GMRES for fluid analysis [Tezduyar (2006)]. Furthermore, partitioned methods can utilize existing parallel analysis codes such as ADVENTURE systems [Yoshimura, Shioya, Noguchi and Miyamura (2002)] and large scale analyses are available without further implementation efforts. However, the partitioned methods were regarded as being not so robust [Causin, Gerbeau and Nobile (2005)] and accurate [Bathe, Zhang and Ji (1999)] compared to the monolithic approaches in case that the solution is carried out without convergence in each time step.

Recently, tightly coupled partitioned methods have been developed using a block Gauss-Seidel approach [Wall, Genkinger and Ramm (2007)] and a block Newton approach [Matthies and Steindorf (2003)][Fernandez and Moubachir (2005)]. Conventional serial staggered schemes solve solid and fluid problems only once in each time step, while the tightly coupled partitioned methods solve those problems iteratively within a fixed time step until satisfying the continuity of interface velocities and tractions. These tightly coupled methods offer the possibility to achieve the same results as the monolithic methods in a robust manner.

A new iterative partitioned coupling algorithm for FSI problems is proposed in this paper. In the

[1] The University of Tokyo, Bunkyo, Tokyo, JAPAN

proposed approach, non-linearity of FSI problems is mainly treated on the interface between solid and fluid portions using the line search method, which minimizes the non-equilibrated displacements on the interface in each fixed point iteration to improve the robustness and efficiency of computation. Performance of the proposed approach is investigated on the flapping motion of MAV, which are inch-size flying robots and have drawn a great deal of attentions for the application of environmental monitoring and life-saving activities. Flapping MAV attracts more attentions than that with fixed wing, because small scale flapping wings could offer superior flight abilities to fixed wings [Mueller (2001)] owing to their unsteady aerodynamics properties. The FSI analysis of the flapping motion of MAV is quite challenging because it requires not only the tight coupling approach to predict flight ability accurately, but also the robust mesh control to trace the large motion of the wing with elastic deformation. Two-dimensional analysis of flapping wing is conducted in this paper to know the performance of the proposed method and the feasibility of large scale three-dimensional analysis of flapping wing.

The fundamental equations for the FSI problems are given in the following section. In the third section, the line search partitioned approach is described. Some numerical examples are given in the forth section. The concluding remarks are given in the final section.

2 Fundamental equations for fluid-structure interaction problems

2.1 Equations for computational solid dynamics

For a structural part, the total Lagrangian description is employed. The equilibrium equation for structural motion and deformation in the domain of structural analysis, Ωs is described as follows;

$$\rho^s \frac{\partial^2 \mathbf{d}^s}{\partial t^2} - \nabla \cdot \mathbf{S}^s = \rho^s \mathbf{b} \quad \text{in } \Omega s \tag{1}$$

where, ρ^s, $\mathbf{S}^s$, $\mathbf{d}^s$, $\mathbf{b}$ denote the mass density, the second Piola-Kirchhoff stress tensor, the displacement vector of structure and the body force vector, respectively. The superscript s stands for the structural component. The second Piola-Kirchhoff stress tensor can be converted to the Cauchy stress tensor σ^s by using material deformation gradient. Boundary conditions are described on Dirichlet boundary, Γ_D^s and Neumann boundary, Γ_N^s as follows;

$$\mathbf{d}^s = \mathbf{d}^{given} \quad \text{on } \Gamma_D^s \tag{2}$$

$$\mathbf{n}^s \cdot \mathbf{S}^s = \mathbf{h}^{given} \quad \text{on } \Gamma_N^s \tag{3}$$

where $\mathbf{n}^s$, $\mathbf{h}^{given}$ represent the outward normal vector and the given force vector, respectively.

Quadrilateral finite element with selective reduced integration is adopted for spatial decomposition. Although large deformation of the structure requires the treatment of geometrical nonlinearity, strains are considered to be infinitesimally small in this research, and hence only linear elastic material is considered.

2.2 Equations for computational fluid dynamics

The incompressible, isothermal, isotropic Newtonian flow governing laminar flow is considered. To follow the structural motion, the Navier Stokes equations with ALE(Arbitrary Lagrangian Eulerian) description is applied for computational fluid dynamics. The primitive variables are velocity $\mathbf{u}^f$ and kinematic pressure $\mathbf{p}^f$.

$$\rho^f \frac{\partial \mathbf{u}^f}{\partial t} + \rho^f (\mathbf{u}^f - \hat{\mathbf{u}}^f) \cdot \nabla \mathbf{u}^f - \nabla \cdot \mathbf{p}^f = \mathbf{f} \quad \text{in } \Omega_f \tag{4}$$

$$\nabla \cdot \mathbf{u}^f = 0 \quad \text{in } \Omega_f \tag{5}$$

The superscript f stands for the fluid component and ρ^f, $\hat{\mathbf{u}}^f$ denote the mass density and the velocity vector of the mesh deformation, respectively. The whole set of equations is defined on a bounded domain Ω_f with boundary Γ, which can be split into its complementary subsets denoted as Dirichlet boundary, Γ_D^f and Neumann boundary, Γ_N^f. The Dirichlet boundary is also decomposed into two subsets denoted as fluid-structure interface, $\Gamma_D^{Interface}$ and only fluid Dirichlet boundary, Γ_D^f.

$$\mathbf{u}^f = \hat{\mathbf{u}}^f \quad \text{on } \Gamma_D^{Interface} \tag{6}$$

$$\mathbf{u}^f = \mathbf{u}^{given} \quad \text{on } \Gamma_D^f \tag{7}$$

$$\mathbf{n}^f \cdot \sigma^f = \mathbf{h}^{given} \quad \text{on } \Gamma_N^f \tag{8}$$

where $\mathbf{n}^f$, σ^f, $\mathbf{h}^{given}$ represent the outward normal vector, stress tensor and given force vector, respectively.

Two kinds of stabilization methods, the streamline upwind/Petrov Galerkin method (SUPG) and the pressure stabilized/Petrov Galerkin method (PSPG) are applied [Tezduyar and Osawa (2000)]. The linear triangular finite element for both pressure and velocity (P1-P1) is adopted for spatial discretization of the analysis domain

2.3 Interaction conditions on fluid-structure interface

The interaction conditions on the fluid-structure interface are described as follow;

$$\sigma^f \cdot \mathbf{n}^f + \sigma^s \cdot \mathbf{n}^s = \mathbf{0} \quad \text{on } \Gamma_D^{Interface} \tag{9}$$

$$\mathbf{u}^f = \mathbf{u}^s = \frac{\partial \mathbf{d}^s}{\partial t} \quad \text{on } \Gamma_D^{Interface} \tag{10}$$

Equation (9) is for equilibrium on the interface, while equation (10) is for geometrical compatibility on the interface. In the iterative partitioned method, the fluid analysis and the solid one are performed iteratively in each fixed time step until they satisfy the above interaction conditions. Such iterative step is referred to as fixed point iteration.

The consistent spatial discretization on the interface can not be expected in the usual problems, and hence special techniques to connect inconsistent meshes are required [Ahren, Beckert and Wendland (2006)]. In this paper, the consistency of the meshes on the interface is assumed to simplify the problems.

2.4 Time integration scheme

For partitioned FSI analyses, the time integration scheme for computational solid dynamics and fluid one can be treated and implemented independently. However, consistent implicit time integration schemes are required for accurate as well as robust analyses[Rugonyi and Bathe (2001)]. In this paper, Newmark's β method is applied in computational solid dynamics, while the backward Euler method is applied for computational fluid dynamics because of its well-tested popularity.

2.5 Mesh control

A robust mesh control is implemented to well describe the large deformation of fluid domain enforced by the flapping motion of the wing. Many smoothing schemes have been proposed to prevent the deterioration of mesh quality as the total displacement of the structure increases [Rugonyi and Bathe (2001)][Degand and Farhat (2002)]. A pseudo elastic smoothing scheme with Jacobian based stiffening [Stein, Tezduyar and Benny (2004)] and a re-connecting procedure with the constrained Delaunay method [Gerorge, Hecht and Saltel (1991)] are adopted as mesh control procedures because of its simple implementation. In the pseudo elastic smoothing, the mesh deformation of fluid domain is virtually governed by the linear elastic equations, and the stiffness of each element is controlled with Jacobian based stiffening approach to avoid distorted tiny elements in the vicinity of the structure. The Jacobian based stiffening is a method to stiff each element according to its area, i.e. the Jacobian in triangular element. Young's modulus of each element can be defined as follows;

$$E_e = E_o (J_e)^{\chi} \tag{11}$$

where E_e, E_0, J_e,χ are Young's modulus of element e, the global Young's modulus, Jacobian of element e and stiffness parameter, respectively. When χ is unity, the element becomes stiff in proportion to its area.

As boundary conditions for pseudo elastic fluid domain, forced displacements are given onto the fluid-structure interface, and fixed nodes are given onto the outer boundaries. Even with this smoothing procedure, the distortion of the mesh is inevitable for the analysis of flapping wing, and hence the re-connecting procedure is introduced as well. The remeshing procedure can be categorized into two processes. The one is a renoding process, [Nishioka, Kobayashi and Fujimoto (2007)] in which nodes are newly gener-

ated in the analysis domain appropriately according to the current geometry. The other is a re-connecting process, where given nodes are connected again according to the given node distribution with an automatic mesh generation procedure such as the constrained Delaunay method. In the present study, only the re-connecting process is adopted as a basic remeshing procedure. The re-connecting process is only applied when the distortion of the element is sufficiently large in terms of inverse element height aspect ratio given as follows;

$$\frac{2}{\sqrt{3}}\frac{\max(edge)}{\min(height)} > \varepsilon_{Distortion} \tag{12}$$

where max(edge) denotes the length of edge which has the maximum length among three edges of the triangular element, and min(height) is the minimum height of the triangle which is defined as the height when the edge with the maximum length is regarded as the base of triangle. This criterion is scaled so that the regular triangle can have the value of unity.

3 Iterative partitioned approach

3.1 Partitioned Approach

The deformation of structure is required as an input data for mesh smoothing scheme and velocity vector of the mesh is obtained for further fluid dynamics analysis. This smoothing procedure can be represented by the function $\mathbf{M}$.

$$\hat{\mathbf{u}}^f = \mathbf{M}(\mathbf{d}^s) \tag{13}$$

For fluid analysis, the required input data is the velocity of the mesh, while the output data for next solid analysis is fluid force on the interface. This procedure can be represented by the function $\mathbf{F}$.

$$\mathbf{f}^f = \mathbf{F}(\hat{\mathbf{u}}^f) \tag{14}$$

Finally, the fluid force can be taken into account in the solid analysis to obtain the structural displacement and the function $\mathbf{S}$ can represent this procedure.

$$\mathbf{d}^s = \mathbf{S}(\mathbf{f}^f) \tag{15}$$

Because the partitioned approach performs the above procedures sequentially, it is difficult to satisfy the geometrical compatibility condition and equilibrium condition on the interface of FSI problem. Since the serial staggered method solves these equations only once typically with structural predictor to have approximation of structural displacement for equation (13), all the obtained results have no guarantee of accuracy. In iterative partitioned approaches, equations (13), (14) and (15) are solved iteratively until it can guarantee the accuracy of the analysis with defined criterion. At nth fixed point iteration, equations (13), (14) and (15) are written as follows;

$$\hat{\mathbf{u}}_n^f = \mathbf{M}(\mathbf{d}_n^s) \tag{16}$$

$$\mathbf{f}_n^f = \mathbf{F}(\hat{\mathbf{u}}_n^f) \tag{17}$$

$$\mathbf{d}_{n+1}^s = \mathbf{S}(\mathbf{f}_n^f) \tag{18}$$

As given in the following criterion, the convergence of the fixed point iteration is judged with sufficiently small value, ε in terms of normalized Euclid norm of non-equilibrated force;

$$\frac{\left|\mathbf{f}_{n+1}^f - \mathbf{f}_n^f\right|}{\left|\mathbf{f}_{n+1}^f\right|} \prec \varepsilon \tag{19}$$

This simple iterative approach is so-called block Gauss Seidel method. It is known that the convergence rate of this approach is quite slow and unstable in case that the mass density of fluid is similar to that of solid [Causin, Gerbeau and Nobile (2005)]. To overcome such an unstable convergence problem, the relaxed Block Gauss Seidel method, where under-relaxation of the structural response is introduced so that an added mass effect is virtually taken into account. Even in the relaxed method, the convergence rate is not so well improved. The inexact or exact Newton method is also introduced [Matthies and Steindorf (2003)][Fernandez and Moubachir (2005)] to overcome the slow convergence rate of the partitioned methods, though they require major changes in the analysis codes because of necessity of the Jacobian matrix.

3.2 Line Search Approach

The line search approach is introduced in this paper to accelerate the convergence of fixed point iteration. Non-equilibrated displacements at nth and $n+1$th fixed point iterations are defined as follows;

$$\mathbf{r}_n^s = \mathbf{d}_{n+1}^s - \mathbf{d}_n^s \tag{20}$$

$$\mathbf{r}_{n+1}^s = \mathbf{d}_{n+2}^s - \mathbf{d}_{n+1}^s \tag{21}$$

Direct application of the non-equilibrated displacements could cause excessive deformation in FSI problems because so-called added mass effect is not taken into account in the computational solid dynamics analysis. Hence, in the relaxed block Gauss-Seidel method, relaxed displacement is applied, when the displacements of structure are updated, for the improvement of stability in fixed point iterations. The relaxed displacements can be given as follows;

$$\mathbf{d}_{n+2}^{s\ relaxed} = \mathbf{d}_{n+1}^s + \lambda \mathbf{r}_{n+1}^s \tag{22}$$

where λ is the constant parameter given by a user. The parameter, λ, should be small enough for stability, however too small λ spoils its convergence rate.

In the line search partitioned approach, λ is computed inside codes automatically. The linear interpolation of the non-equilibrated displacements between nth and $n+1$th fixed point iterations can be described as follow;

$$\mathbf{r}_{\text{interpolated}}^s = (1-\alpha)\mathbf{r}_n^s + \alpha \mathbf{r}_{n+1}^s \tag{23}$$

A schematic view of the line search approach in one-dimensional example is shown in Fig.1. The minimization of linearly interpolated non-equilibrated displacements can be given by the parameter, α, in the following;

$$\alpha = \arg\min\left(\left|(1-\alpha)\mathbf{r}_n^s + \alpha \mathbf{r}_{n+1}^s\right|\right) \tag{24}$$

Finally the optimal displacements of the structure, which minimizes non-equilibrated displacements, can be described as follows;

$$\mathbf{d}_{Optimal}^s = (1-\alpha)\mathbf{d}_n^s + \alpha \mathbf{d}_{n+1}^s + \beta\left\{(1-\alpha)\mathbf{r}_n^s + \alpha \mathbf{r}_{n+1}^s)\right\} \tag{25}$$

where $\beta (0 < \beta \leq 1.0)$ must be given by the user yet. β has a small effect on the convergence, compared to α. β is introduced to avoid the situation such that the optimal parameter is searched only on one line as shown in Fig.2.

The non-linear loop in each fluid analysis and that of solid analysis can be treated in the loop of fixed point iteration because the line search method is one of traditional non-linear analysis schemes. The original fluid-structure interaction analysis procedure with the line search partitioned approach is described in Fig.3. The non-linear problem in each fluid problem and that of solid problem are treated independently inside each analysis code. Since there is an iteration loop over the fluid-structure interaction, the non-linearity for fluid and solid problems could be treated in this loop of fixed point iteration as shown in Fig.4. In this paper, the original analysis scheme shown in Fig.3 is referred to as two loops approach, while alternative approach shown in Fig.4 is referred to as one loop approach.

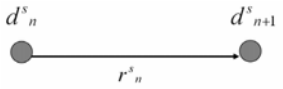

(a) non-equilibrated displacement at nth fixed point iteration

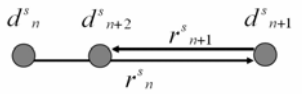

(b) non-equilibrated displacement at $n+1$th fixed point iteration

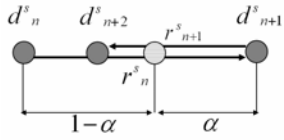

(c) interpolated displacement with parameter α

Figure 1: Schematic view of one dimensional line search method

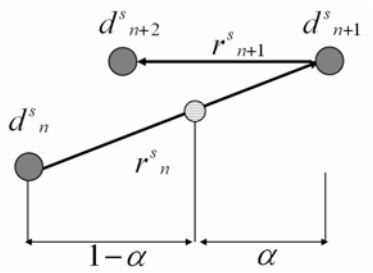

(a) interpolated displacements with only α

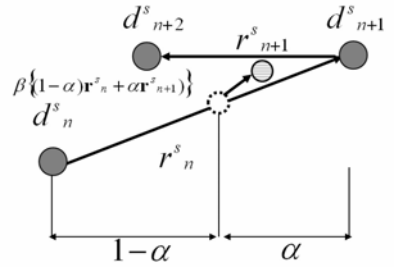

(b) interpolated displacements with α and β

Figure 2: Schematic view of two dimensional line search method

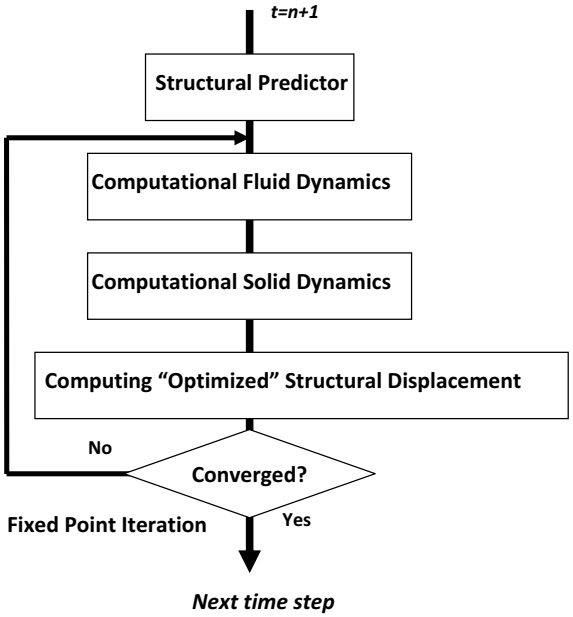

Figure 4: One loop partitioned approach

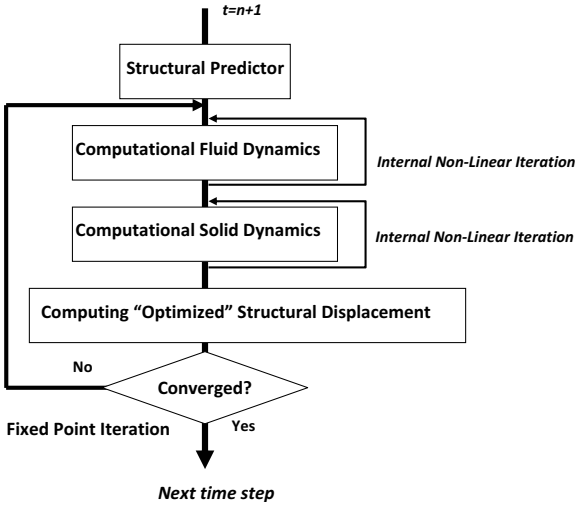

Figure 3: Two loops partitioned approach

4 Numerical examples

4.1 Vortex-induced oscillations of flexible structure in the wake of a bluff body

The first numerical example is introduced to show the performance of the present approach. This example was employed by many researchers to demonstrate the stability of their monolithic and partitioned methods. The vortices induced by flows around rigid bluff body cause structural oscillations of the plate, which fixed at the downstream end of the bluff body. The geometry of the analysis domain and its boundary conditions are given in Fig.5. The material properties of the fluid and the structure are the same as those employed in Wall's research [Wall and Ramm (1998)]. Young's modulus, Poisson's ratio and mass density of the structure are $2.5\times10^5 g/mm\cdot s^2$, 0.35, $1.0\times10^{-4}g/mm^3$, respectively. The viscosity and mass density of the fluid are, $1.82\times10^{-5}g/mm\cdot s$, $1.18\times10^{-6}g/mm^3$, respectively. The inflow velocity is U=513mm/s, which results in Re =333. The geometrical configurations are D=10mm and h=0.6mm. The number of triangular finite elements and that of nodes in the fluid analysis domain are 41,050 and 20,935, respectively, while the number of quadrilateral finite elements and that of nodes in the solid analysis domain are 1,200, and 1,407, respectively. The structure has six elements in the thickness direction. The time step size is $5.0\times10^{-4}s$. For the purpose of comparison, the block Gauss-Seidel approach and relaxed block Gauss-Seidel approach with dynamics computation of relaxation parameter by using Aitken method [Wall, Genkinger and Ramm (2007)] are conducted. Aitken method is one

of the most efficient dynamics computation approaches of relaxation parameter α.

The time history of vertical displacement on the tip of elastic plate is given in Fig.6. Some typical flow patterns around the elastic plate are given in Fig.7. The amplitude of the quasi stationary oscillation is approximately in between 11mm to 12.5mm, and the average frequency of this oscillation is approximately 3.2Hz. These numerical results agree well with other researchers' results. The transient oscillation before reaching quasi stationary motion, i.e. from 0.0sec. to 2.0sec., quite resembles the result in [Dettmer and Peric (2006)]. The numbers of fixed point iterations and computation times until 10,000th time step on Pentium 4 3.0GHz for all analysis cases are summarized in table 1. All the combinations of approaches give the same numerical results. It is clearly shown in the table that the one loop line search approach reduces 33% of computation time compared to the two loops approach with the relaxed block Gauss-Seidel method and as efficient as the Aitken method. In this example, mesh distortion was not so significant and thus the reconnecting procedure was not invoked throughout the analysis.

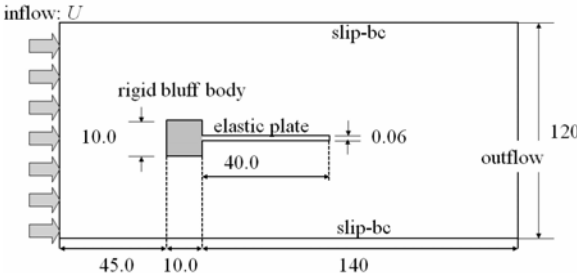

Figure 5: Geometry and boundary conditions

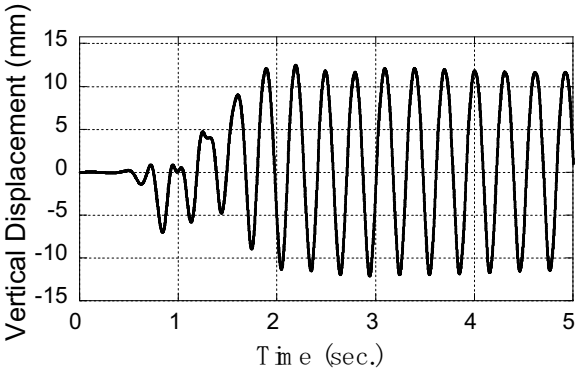

Figure 6: Time history of vertical displacement on the tip of the flexible plate

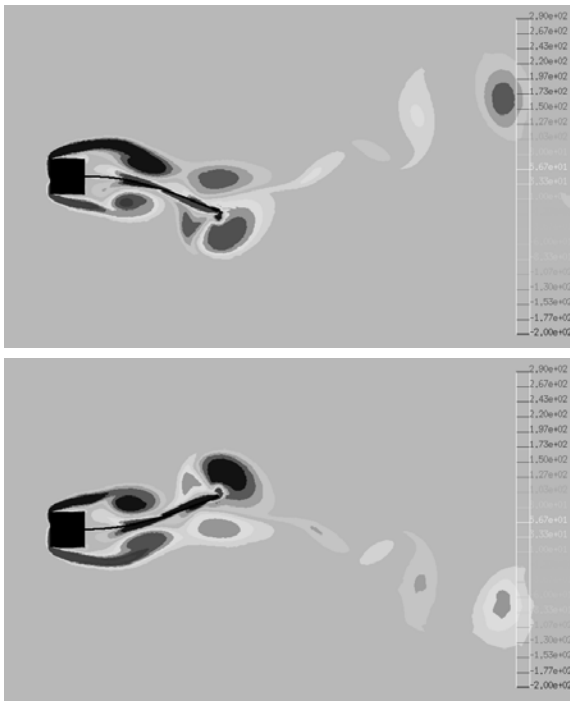

Figure 7: Vorticity Distributions around flexible plate

4.2 Flapping Motion of a Flexible Wing

Flapping motion of flexible wing was analyzed as a simplified two-dimensional problem. The length of wing chord is 5.0mm and the thickness is 0.08mm. The motion of wing consists of flapping and feathering motion as shown in Fig.8. The fluid properties are the same as those of the previous example. Flapping motion prescribed at the leading edge of the wing ranges from –2.5mm to +2.5mm and that of feathering angle ranges from –45 degrees to +45 degrees. 200Hz is set for the flapping and feathering frequencies. Young's modulus, Poisson's ratio, and mass density of the structure are$1.0 \times 10^8 g/mm^2 \cdot s$, 0.2, $5.0 \times 10^{-5} g/mm^3$, respectively. The number of triangular finite elements and that of nodes in fluid analysis domain are 48,044 and 24,316, while the

Table 1: Numbers of fixed point iterations and computation times

Loop Treatment	Under-relaxation scheme	Averaged number of fixed point iterations	Computation time (hours)
Two loops	Block Gauss-Seidel	12.1	117
	Aitken	6.21	73.5
	present	6.03	72.2
One loop	Block Gauss-Seidel	13.3	64.2
	Aitken	6.44	39.9
	present	6.33	39.1

number of quadrilateral finite elements and that of nodes in the solid analysis domain are 1,000, and 1,255. The time step size is 1.0×10^{-6} sec.

A leading edge vortex, which produces unsteady lift flight force for flapping motion [Dickinson, Lehmann and Sane (1999)] was observed. The deformations of the wing and pressure distributions in prescribed flapping and feathering motion are shown in Fig.9. To investigate the effect of elastic deformation of the wing, only flapping motion is prescribed at the leading edge of the wing as a boundary condition in the solid analysis. The elastic deformations of the wing and pressure distributions around the flexible wing are shown in Fig.10. The comparison between Figs.9 and 10 clearly shows that even without prescribed feathering motion, the elastic deformation of the flexible wing can produce passive feathering motion, though the angle of feathering is not so enough compared with that of prescribed feathering motion. Owing to such passive feathering motion, lift forces are generated as shown in Fig.11. It should be noted here that the flapping motion of rigid wing, which is symmetric in the vertical direction, produces no lift force. Further research must be conducted to compare the efficiency of fish and insect motion in terms of material properties and the definition of flapping motion.

Time histories of the mesh distortion defined in equation (12) with or without re-connecting scheme are shown in Fig.12. The flapping motion of the wing inevitably produces large deformation of the fluid domain. Only employing the smoothing procedure results in break down of computation, while the combined utilization of re-connecting and smoothing procedures works well. The re-connecting criterion $\varepsilon_{Distortion}$ is 10.8 in this computation.

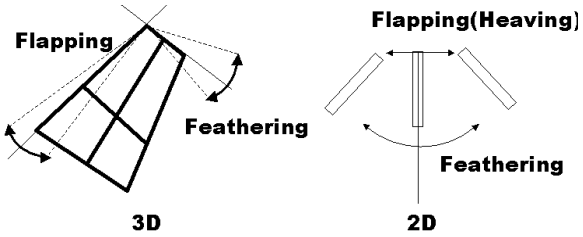

Figure 8: Schematic view of wing motion

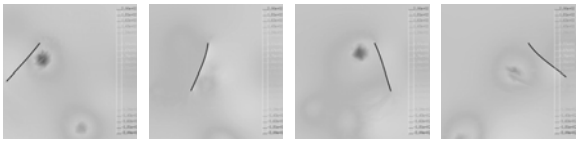

Figure 9: Elastic deformation of the wing with feathering motion (up stroke, right to left)

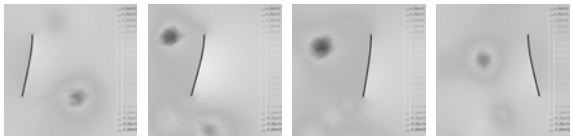

Figure 10: Time histories of lift force

5 Concluding remarks

To improve accuracy and stability of partitioned fluid structure interaction analysis procedures, a line search partitioned coupling approach was newly proposed in this paper. The line search

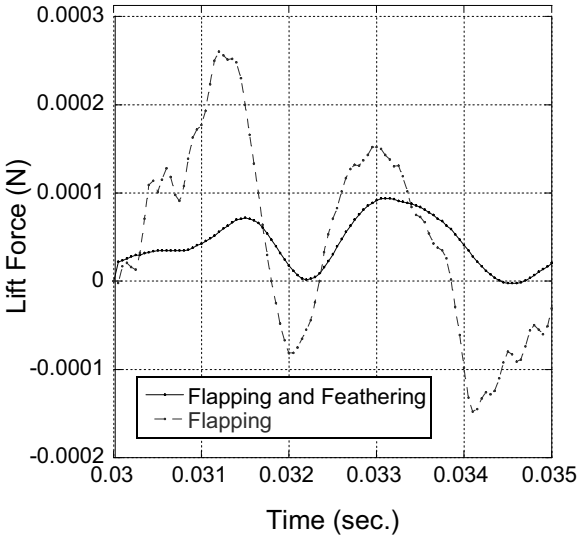

Figure 11: Elastic deformation of the wing without prescribed feathering motion (up stroke, right to left)

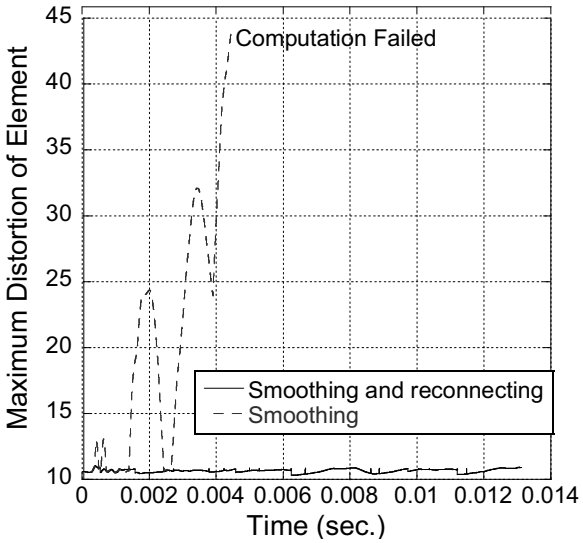

Figure 12: Time histories of mesh distortion

method obtains the optimal relaxation parameter, which minimizes the non-equilibrated displacements. In addition, one loop iterative partitioned approach and robust mesh control schemes with smoothing and re-connecting were implemented. Using these methods, the computation cost of analyzing flexible structure in the wake of a bluff body was 33% reduced and the flapping motion of flexible wing was analyzed successfully. It is clearly shown from the FSI analyses that the elastic deformation of the flapping wing can produce passive feathering motion and generate lift force effectively.

Acknowledgement: The present research was supported in part through the 21st Century COE Program, "Mechanical Systems Innovation," by the Ministry of Education, Culture, Sports, Science and Technology.

References

Ahrem, R.; Bechert, A.; Wendland, H. (2006): A meshless spatial coupling scheme for large-scale fluid-structure-interaction problems. *CMES: Computer Modeling in Engineering and Sciences*, vol. 12, pp. 121-136.

Bathe, K. J.; Zhang, H.; Ji, S. (1999): Finite element analysis of fluid flows fully coupled with structural interactions. *Computers and Structures*, vol. 72, pp. 1-16.

Causin, P.; Gerbeau, J.F.; Nobile, F. (2005): Added-mass effect in the design of partitioned algorithms for fluid–structure problems. *Computer Methods in Applied Mechanics and Engineering*, vol. 194, pp. 4506-4527.

Degand, C.; Farhat, C. (2002): A three-dimensional torsional spring analogy method for unstructured dynamics meshes. *Computers and Structures*, vol. 80, pp. 305-316.

Dettmer, W.; Peric, D. (2006): A computational framework for fluid-structure interaction: Finite element formulation and applications. *Computer Methods in Applied Mechanics and Engineering*, vol. 195, pp. 5754-5779.

Dickinson, M.H.; Lehmann, F.O.; Sane, S.P. (1999): Wing rotation and the aerodynamic basis of insect flight. *Science*, vol. 284, pp. 1954-1960.

Fernandez, M.A.; Moubachir, M. (2005): A Newton method using exact jacobians for solving fluid-structure coupling. *Computers and Structures*, vol. 83, pp. 127-142.

Gardano, P.; Dabnichki, P. (2006): Application of boundary element method to modelling of added mass and its effect on hydrodynamic

forces. *CMES: Computer Modeling in Engineering and Science*, vol. 15, pp. 87-98.

George, P.; Hecht, F.; Saltel, E. (1991): Automatic mesh generation with specified boundary. *Computer Methods in Applied Mechanics and Engineering*, vol. 92, pp. 269-288.

Ishihara, D.; Yoshimura, S. (2005): A monolithic approach for interaction of incompressible viscous fluid and an elastic body based on fluid pressure Poisson equation. *International Journal of Numerical Methods in Engineering*, vol. 64, pp. 167-203.

Mandel, J. (1993): Balancing domain decomposition. *Communication on Numerical Methods in Engineering*, vol.9, pp.233-241, 1993.

Matthies, H.G.; Steindorf, J. (2003): Partitioned coupling algorithms for fluid-structure interaction. *Computers and Structure*, vol. 81, pp. 805-812.

Mueller, T.J. (2001): Fixed and flapping wing aerodynamics for micro air vehicle applications. *American Institute of Aeronautics and Astronautics*, pp. 6-7.

Nishioka, T.; Kobayashi, Y.; Fujimoto, T. (2007): The moving finite element method based on Delaunay automatic triangulation for fracture path prediction simulations in nonlinear elastic-plastic materials. *CMES: Computer Modeling in Engineering and Science*, vol. 17, pp. 231-238.

Rugonyi, S.; Bathe, K.J. (2001): On finite element analysis of fluid flows fully coupled with structural interactions. *CMES: Computer Modeling in Engineering and Sciences*, vol. 2, pp. 195-212.

Schenato, L.; Wu, W.C.; Sastry, S.S. (2004): Attitude control for a micromechanical flying insect via sensor output feedback. *IEEE Journal of Robotics and Automation*, vol. 20, no. 1, pp. 93-106.

Stein, K; Tezduyar, T.E.; Benny, R. (2004): Automatic mesh update with the solid-extension mesh moving technique. *Computer Methods in Applied Mechanics and Engineering*, vol. 193, pp. 2019-2032.

Tezduyar, T.E. (2006): Interface-tracking and interface-capturing techniques for finite element computation of moving boundaries and interfaces. *Computer Methods in Applied Mechanics and Engineering*, vol. 195, pp. 2983-3000.

Tezduyar, T.E.; Osawa Y. (2000): Finite element stabilization parameters computed from element matrices and vectors. *Computer Methods in Applied Mechanics and Engineering*, vol. 190, pp. 411-430.

Wall, W.A.; Genkinger, S.; Ramm, E. (2007): A strong coupling partitioned approach for fluid-structure interaction with free surfaces. *Computers and Fluids*, vol. 36, pp. 169-183.

Wall, W.A.; Ramm, E. (1998): Fluid–structure interaction based upon a stabilized (ALE) finite element method. *Proceedings of the 4th World Congress on Computational Mechanics New Trends and Applications*, CD-ROM, CIMNE.

Yang, C.; Tang, D.; Yuan, C.; Hatsukami, T.; Zheng, J.; Woodard, P. (2007): In Vivo/Ex Vivo MRI-based 3D non-newtonian FSI models for human atherosclerotic plaques compared with fluid/wall-only models. *CMES: Computer Modeling in Engineering and Science*, vol. 19, pp. 233-245.

Yoshimura, S.; Shioya, R.; Noguchi, H.; Miyamura, T. (2002): Advanced general-purpose computational mechanics system for large-scale analysis and design. *Journal of Computational and Applied Mathematics*, vol. 49, pp. 279-296.

Zhang, Q.; Hisada, T. (2001): Analysis of fluid-structure interaction problems with structural buckling and large domain changes by ale finite element method. *Computer Methods in Applied Mechanics and Engineering*, vol. 190, pp. 6341-6357.